

## VLT OBSERVATIONS OF THE ULTRALUMINOUS X-RAY SOURCE NGC 1313 X-2

P. MUCCIARELLI<sup>1,2</sup>, L. ZAMPIERI<sup>2</sup>, R. FALOMO<sup>2</sup>, R. TUROLLO<sup>3</sup> AND A. TREVES<sup>4</sup>*Draft version August 11, 2018*

## ABSTRACT

We present archive ESO VLT photometric and spectroscopic data of the Ultraluminous X-ray source NGC 1313 X-2. The superb quality of the VLT images reveals that two distinct objects, with  $R$  magnitudes 23.7 and 23.6, are visible inside the *Chandra* error box. The two objects, separated by  $0.75''$ , were unresolved in our previous ESO 3.6 m+EFOSC image. We show that both are stars in NGC 1313, the first a B0-O9 main sequence star of  $\sim 20M_{\odot}$ , while the second a G supergiant of  $\sim 10M_{\odot}$ . Irrespectively of which of the two objects the actual counterpart is, this implies that NGC 1313 X-2 is a high mass X-ray binary with a very massive donor.

*Subject headings:* galaxies: individual (NGC 1313) — stars: individual (NGC 1313 X-2) — X-rays: binaries — X-rays: galaxies

## 1. INTRODUCTION

First revealed by *Einstein*, the population of ultraluminous X-ray Sources (ULXs) has increasingly grown up in the last decade mainly thanks to the observations of *ROSAT* (e.g. Colbert & Ptak 2002), *XMM-Newton* (e.g. Foschini et al. 2002a) and *Chandra* (e.g. Liu & Bregman 2005a; Swartz et al. 2004). About 150 ULXs are included in the recent *Chandra* catalogue of Swartz et al. (2004). These point-like sources have X-ray luminosities  $L_X \gtrsim 10^{39}$  erg s<sup>-1</sup>, in excess of that of a  $\sim 10M_{\odot}$  compact object accreting at the Eddington limit. Variability in the X-ray flux on timescales of months is observed in about half of the *ROSAT* ULXs with multiple observations (Colbert & Ptak 2002), while about 5-15% of the *Chandra* ULXs show variability during a single observation (average exposure time  $\sim 40$  ks, Swartz et al. 2004).

For several sources with sufficiently good statistics, the best fit to the X-ray spectrum is obtained with a two-component model, a soft multicolor disk (MCD) blackbody plus a power law. Some ULXs show typical temperatures of the MCD component 5-10 times lower than those of Galactic X-ray binaries. The high luminosity, the very soft thermal component (if it represents the emission from a cool accretion disk) and the variability suggest that these sources may be powered by accretion onto an Intermediate Mass Black Hole (IMBH) of 100-1000  $M_{\odot}$ . Nevertheless, many of the ULX properties can be explained if they do not emit isotropically (King et al. 2001) or are dominated by emission from a relativistic jet (e.g. Kaaret et al. 2003). In this case, they may harbor stellar mass BHs and may be similar to Galactic black hole binaries.

Multiwavelength observations are definitely a powerful tool to investigate the nature of ULXs. Radio emission, when present, gives important clues on the geometry, energetics and lifetime of ULXs (Kaaret et al. 2003; Miller et al. 2005). Optical follow-ups are crucial to identify ULX counterparts and clean up the population from the significant contamination of background AGNs and interacting

SNe (Foschini et al. 2002b; Masetti et al. 2003; Swartz et al. 2004). Up to now only a very small number of ULXs have been convincingly associated with stellar objects of known spectral type (e.g. Liu et al 2002, 2004; Kaaret et al. 2004). All these ULXs are hosted in star-forming regions and their optical counterparts have properties consistent with those of early type O-B stars. Some ULXs are also associated with extended optical emission nebulae (Pakull & Mirioni 2002).

NGC 1313 X-2 is a prototypical ULX (see Miller et al. 2003; Zampieri et al. 2004; Turolla et al. 2005, and references therein). With a luminosity  $L_X \sim 10^{40}$  erg s<sup>-1</sup> in the 0.2-10.0 keV band, it is a good candidate for harboring an IMBH ( $M \gtrsim 100M_{\odot}$ ). Such an option is corroborated by the presence of a very soft X-ray spectral component ( $T \sim 200$  eV) which points to a compact object of mass definitely larger than those of Galactic Black Hole candidates. Moreover, the object exhibits X-ray variability on a timescale of months.

On the basis of a 19 ks *Chandra* exposure and accurate astrometry of field objects, Zampieri et al. (2004) (Z04 hereafter) derived the source position with an uncertainty of  $0.7''$  (RA=03:18:22.34, DEC=-66:36:03.7;  $1\sigma$  confidence level). Inside the *Chandra* error box a faint optical candidate was found on a R band image taken with the ESO 3.6 m telescope in January 2002.

Here we present a follow-up study of the optical counterpart of NGC 1313 X-2, based on photometric archive data obtained with the ESO VLT telescope and a reconsideration of our previous photometry of the ESO 3.6 m+EFOSC image.

## 2. OPTICAL OBSERVATIONS: DATA REDUCTION AND ANALYSIS

We analyzed archive ESO VLT+FORs1 images (*BVR*) and spectra of NGC 1313 X-2 taken between December 2003 and January 2004 (Program ID 072.D0614). The observations are listed in Table 1. Data reduction was

<sup>1</sup> Department of Astronomy, University of Padua, Vicolo dell'Osservatorio 2, I-35122 Padova, Italy; mucciarelli@pd.astro.it

<sup>2</sup> INAF-Astronomical Observatory of Padua, Vicolo dell'Osservatorio 5, I-35122 Padova, Italy; zampieri@pd.astro.it, falomo@pd.astro.it

<sup>3</sup> Department of Physics, University of Padua, Via Marzolo 8, I-35131 Padova, Italy; turolla@pd.infn.it

<sup>4</sup> Department of Physics and Mathematics, University of Insubria, Via Valleggio 11, I-22100 Como, Italy; treves@mib.infn.it

performed using standard IRAF<sup>5</sup> procedures. The images were astrometrically calibrated using 29 GSC2 stars. The calibration uncertainty, tested with GSC2 stars not used for the calibration, is  $\sim 0.3''$ . Finally, for each band the images were combined and cleaned from cosmic rays. Figure 1 shows the combined  $R$  and  $B$  images. On the same night a short exposure of the standard PG 0231+051 Landolt field (Landolt 1992) was also taken in each band. Aperture photometry ( $1''$  radius) was performed on the combined images. The instrumental magnitudes were then calibrated with the Landolt standard stars in the Bessel-Cousins system (see Patat 2003, for extinction coefficients and color terms).

Z04 give the  $R$  magnitude of a number of objects around NGC 1313 X-2 and of the proposed counterpart (object C in their paper). The latter was close to the limit of detectability on their image and appeared as a single object. Thanks to the higher resolution of the VLT image, in the  $R$  and  $V$  exposures we are able to resolve object C in two distinct point sources, C1 and C2. Both are inside the *Chandra* error box (see Figure 1). Object C2 is not detected in the  $B$  band frame. Magnitudes, colors and astrometric positions of the two candidate counterparts, C1 and C2, and of objects A, B, and D (following Z04) are reported in Table 2. The photometric errors are the  $2\sigma$  statistical errors on the measurements with the different Landolt standards. For object C2, we quote an upper limit to the  $B$  band magnitude using the plate limit ( $B = 25.2$ ).

The total magnitude of object C1+C2 is  $R = 23.2 \pm 0.05$ . We note that this measurement is not in agreement with the estimated magnitude of object C obtained in our previous ESO 3.6m image ( $R = 21.6$ ; see Z04). In fact, re-analyzing the old image we found that the stellar background used for subtraction was underestimated, leading to a measurement  $\sim 0.3$  mag brighter. We also found a mistake in the adopted exposure time of the image that causes an overestimate of another  $\sim 0.9$  mag. The revised magnitude of object C in the ESO 3.6m image is now found to be  $R = 22.9 \pm 0.2$ , in reasonable agreement (within  $2\sigma$ ) with the VLT measurement.

In addition to the images, we also analyzed four VLT+FORS1 spectra ( $\lambda_c = 5900$  A,  $\lambda/\Delta\lambda = 440$  at  $\lambda_c$ ) of objects C1+C2 taken in different nights (Table 1). The slit ( $1''$ ) was oriented to include object D. After performing standard reduction, all spectra were sky subtracted, wavelength calibrated through comparison lamp exposures and flux calibrated using standard star spectra obtained in the same night. In these VLT+FORS1 spectra the two sources (C1 and C2) are not spatially resolved. The 2D spectrum taken on 15 January 2004 is shown in Figure 2. Nebular emission lines of [OII]  $\lambda$  3727 A,  $H_\gamma$ ,  $H_\beta$ , [OIII]  $\lambda\lambda$  4959-5007 A, [OI]  $\lambda$  6300 and 6364 A,  $H_\alpha$ , [NII]  $\lambda$  6583 A and [SII]  $\lambda\lambda$  6717-6731 A are clearly detected. Note that this is the first detection of a [OII] line from this nebula. A one dimensional spectrum was extracted over an aperture of  $2.2''$  centered on object C1+C2 from each of the four combined spectra. Two nebular spectra were extracted from different  $1''$  apertures, eastward and westward of the source position and adjacent to it. The two spectra were then averaged and the resulting spectrum subtracted from

that of object C1+C2. All these spectra, taken on January 15th, are shown in Figure 3. The nebula-subtracted source spectrum shows no evident emission or absorption lines. Residuals are present in coincidence with some nebular lines (especially [OIII] and  $H_\alpha$ ), with an upper limit to the equivalent width of  $\sim 30$  A. In particular the residual flux in the [OIII] line is a non negligible fraction of the nebular flux. This appears to be caused by an increased emission of the nebular line around the position of object C1+C2. It is not clear if this is simply induced by a change in the rather irregular spatial profile of the nebular line or by a variation of the physical conditions produced by the presence of the nearby ULX. Finally, marginal evidence of an excess in emission may be seen at 4686 A, corresponding to HeII emission, but the line is not statistically significant.

### 3. RESULTS

The superb quality of the VLT images reveals that two distinct objects, C1 and C2, are visible inside the *Chandra* error box of NGC 1313 X-2 in the  $R$  and  $V$  bands. From the astrometric positions reported in Table 2, we infer a separation of  $0.75''$  and a position angle (C2 with respect to C1) of  $\sim 131^\circ$ . Note that the two objects were unresolved in our previous 3.6 m+EFOSC image.

The possibility that either C1 or C2 may be a background AGN appears very unlikely. In fact, no statistically significant emission line at wavelengths longer than  $H_\alpha$  is observed in the optical spectrum nor any other feature that may be identified with a highly redshifted emission line. Furthermore, from the  $R$  magnitude of objects C1 and C2, and the X-ray flux of the last *XMM-Newton* observation ( $f_X \sim 2 \times 10^{-12}$  erg cm<sup>-2</sup> s<sup>-1</sup>; Z04), we obtain a X-ray to optical flux ratio  $f_X/f_R \gtrsim 2000$ . This is more than an order of magnitude larger than the typical value for an AGN ( $\lesssim 100$ ). The possibility that object C2 is a highly obscured AGN is not very convincing either. In fact, to produce the same X-ray flux but a  $f_X/f_R$  ratio of  $\sim 100$ , the  $R$  magnitude should be  $\sim 20$ . Therefore the additional reddening required to make object C2 look like an obscured AGN is  $A_R \simeq 3.5$  mag, corresponding to a column density  $\sim 9 \times 10^{21}$  cm<sup>-2</sup> (Bohlin et al. 1978), much larger than that inferred from X-ray spectral fits [ $\sim (3_{-0.4}^{+0.9}) \times 10^{21}$  cm<sup>-2</sup>]. Unless absorption in NGC 1313 is characterized by an extinction law quite different with respect to that in our Galaxy, we are led to rule out an identification with an (obscured) AGN.

A photometric analysis of a large sample of field stars ( $> 30$ ) was performed on the three  $BVR$  images. A color-color plot of these objects is shown in Figure 4. Almost all of them have stellar colors, apart from two on the lower right part of the diagram that are bluer than ordinary stars. Given their apparent magnitude, objects earlier than spectral type F (including C1) are stars in NGC 1313, while the others may be Galactic foreground stars or belong to NGC 1313. However, object C2 cannot be a Galactic foreground star because its absolute visual magnitude would be  $M_V \sim 9$ , too large to be consistent with its colors.

Within the photometric errors, the colors of object C1

<sup>5</sup> IRAF is distributed by the National Optical Astronomy Observatories, which are operated by the Association of Universities for Research in Astronomy, Inc., under cooperative agreement with the National Science Foundation.

appear to be consistent with those of a A3-O9 I or a A2-B0 V star, while those of C2 with a G8-G7 I star (see e.g. Cox 2000; Braddley 1982). Unfortunately, the optical continuum does not provide useful information for assessing the spectral type because the light from both objects contributes to it. Observationally, the slope of the continuum can be characterized by a power law,  $\lambda^{-1.8}$ . The absence or extreme weakness of the HeII  $\lambda$  4686 Å emission line in the optical spectrum suggests that X-ray irradiation is not dominant. Taking Galactic absorption into account and assuming  $A_V \simeq 0.3$  (Cardelli et al. 1989 extinction law with  $R_V = A_V/E_{B-V} = 3.1$  has been used throughout), the unreddened colors of object C1 are  $(V - R)_0 = -0.2 \pm 0.2$  and  $(B - V)_0 = -0.2 \pm 0.2$ , consistent with those of a B8-O I or A0-O5 V star (see Figure 4). For object C2 it is  $(V - R)_0 = 0.4 \pm 0.2$  and  $(B - V)_0 \gtrsim 1.0$ , consistent only with a G4 I star (see again Figure 4). Recently, Liu et al (2005b) performed a 6.4 m Magellan/Baade observation of the field around NGC 1313 X-2 and found a  $I = 23.3$  mag object in coincidence with the position of C1+C2 (that appear unresolved in their  $I$  frame). Assuming that the flux in the  $I$  band originates mainly from the redder object C2, we then obtain  $(R - I) = 0.3 \pm 0.2$ , consistent with our tentative spectral classification.

At the distance of NGC 1313 ( $d = 3.7$  Mpc; Tully 1988) the  $V$  magnitudes of C1 and C2 (reported in Table 2) translate into the absolute magnitudes  $M_V \sim -4.6$  and  $\sim -4.1$ , respectively. Comparing these values with the absolute magnitudes of main sequence and supergiant stars (e.g. Cox 2000; Braddley 1982), we find that the observed value is consistent only with a B0-09 main sequence star for C1, while it is consistent with a G4 supergiant of type Ib for C2. Therefore, we conclude that both C1 and C2 are stars in NGC 1313, with C1 an early type main sequence star and C2 a supergiant. The bolometric luminosities of the two objects are  $\sim 3 \times 10^{38}$  erg s $^{-1}$  and  $\sim 2 \times 10^{37}$  erg s $^{-1}$ , respectively.

Given the density of objects in the field of view ( $\sim 50 - 100$  arcmin $^{-2}$ ), a significant fraction of which are supergiants in NGC 1313, the probability that C1 or C2 fall by chance inside the  $2\sigma$  *Chandra* error box is not negligible ( $\sim 0.1$ ). However, the chance occurrence of two objects, separated by only  $0.7''$ , inside the X-ray error box is  $\sim 5 \times 10^{-3}$ , sufficiently small to be considered rather unlikely. Actually, if both C1 and C2 are stars in NGC 1313, a physical association may not be unfeasible (the distance corresponding to the apparent separation on the sky is  $\sim 10$  pc). Therefore, we conclude that the ULX is most probably physically associated to either object C1 or C2. Irrespective of which of the two objects is the

actual counterpart, NGC 1313 X-2 appears to be a high mass X-ray binary with a very massive donor star.

We now briefly consider what are the consequences if either C1 or C2 are the counterparts of the X-ray source. A B0-O9 main sequence star has an initial mass of  $\sim 20M_\odot$ . In this respect our analysis essentially confirms the original suggestion by Z04, who proposed that the optical counterpart of NGC 1313 X-2 may be an O type main sequence star in NGC 1313. If the colors are affected by the binary interaction, the estimated mass may vary somewhat. A  $\sim 20M_\odot$  donor star could easily provide the mass transfer rate required to fuel the accreting black hole through Roche-lobe overflow during the main sequence phase if the orbital separation is  $\approx 1$  AU. In these conditions, the mass transfer would be stable and the source persistent (Patruno et al. 2005; Patruno & Zampieri, in preparation).

If object C2 is the counterpart, the nature of the system remains unchanged. In this case X-ray irradiation may be significant and give a non-negligible contribution to the optical emission. The mass corresponding to a G4 supergiant is  $\sim 10M_\odot$ . The same caveat discussed for C1 about the possibility that the colors and mass estimate are affected by binary interaction applies also in this case. The mass transfer rate provided by such a donor star through Roche-lobe overflow is certainly adequate also for large orbital separations. Wind accretion may also be a viable alternative.

At the present stage, there seems to be no compelling argument to rule out any of the two objects C1 and C2 as possible counterparts of NGC 1313 X-2. In both cases, NGC 1313 X-2 is a high-mass X-ray binary with a very massive donor. In order to distinguish which of the two objects is the counterpart, further observations are needed. In particular, we aim at optical spectroscopy under optimal seeing conditions and with the slit along the line connecting C1 and C2, which would allow us to check the existence of typical lines of X-ray binaries (like He II  $\lambda$  4686 Å). Theoretical modelling (binary evolution calculations) may also help distinguish the counterpart. It will also clarify the properties of the accretion flow and the compatibility with the IMBH or stellar black hole interpretations.

Based on observations made with ESO Telescopes at the Paranal Observatories, obtained from the ESO/ST-ECF Science Archive Facility. This work has been partially supported by the Italian Ministry for Education, University and Research (MIUR) under grant PRIN-2004-023189. We thank Alessandro Patruno for interesting discussions on the properties of IMBH binary systems.

## REFERENCES

- Braddley, S., 1982, Numerical data and functional relationships in science and technology, New Series, group VI, vol. 2, Astronomy and Astrophysics, Extension and Supplement to vol. 1, Stars and Star Clusters, Springer
- Cox, A.N. 2000, *Allen's Astrophysical Quantities*, Springer
- Bohlin, R.C., Savage, B.D., & Drake, J.F. 1978, *ApJ*, 224, 132
- Cardelli, J.A., Clayton, G.C. & Mathis, J.S. 1989, *ApJ*, 345, 245
- Colbert, E.J.M., & Ptak, A.F. 2002, *ApJS*, 143, 25
- Foschini, L., et al. 2002a, *A&A*, 392, 817
- Foschini, L., Ho, L.C. & Masetti, N. 2002b, *A&A*, 396, 787
- Kaaret, P., Corbel, S., Prestwich, A.H., & Zezas, A. 2003, *Science*, 299, 365
- Kaaret, P., Ward, M.J., & Zezas, A. 2004, *MNRAS*, 351, 83
- King, A.R. et al., 2001, *ApJ*, 552, 109
- Landolt, A.U. 1992, *AJ*, 104, 340
- Liu, J., Bregman, J.N., & Seitzer, P. 2002, *ApJ*, 580, 31
- Liu, J., Bregman, J.N., & Seitzer, P. 2004, *ApJ*, 602, 249
- Liu, J., & Bregman, J.N. 2005, *ApJS*, 157, 59
- Liu, J., Bregman, J.N., Seitzer, P. & Irwin, J. 2005, astro-ph/0501310
- Masetti, N., et al. 2003, *A&A*, 406, L27
- Miller, J.M., Fabbiano, G., Miller, M.C., & Fabian, A.C. 2003, *ApJ*, 585, 37
- Miller, N.A., Mushotzky, R.F. & Neff, S.G. 2005, *ApJ*, 623, 109

Pakull, M.W., & Mirioni, L. 2002, in Proc. ESA Symp., New Visions of the X-ray Universe in the *XMM-Newton* and *Chandra* Era, eds. F. Jansen et al. (ESA SP-488) (astro-ph/0202488)  
 Patat, F. 2003, *A&A*, 400, 1183  
 Patruno, A., Colpi, M., Faulkner, A. & Possenti, A., 2005, *MNRAS* in press (astro-ph/0507229)

Swartz, D.A., Ghosh, K.K., Tennant, A.F., & Wu, K. 2004, *ApJS*, 154, 519  
 Tully, R.B. 1988, *Nearby Galaxies Catalog* (Cambridge: Cambridge University Press)  
 Turolla, R. et al. 2005, in Proceedings of the 35th COSPAR Scientific Assembly, p. 3749  
 Zampieri, L. et al. 2004, *ApJ*, 603, 523 (Z04)

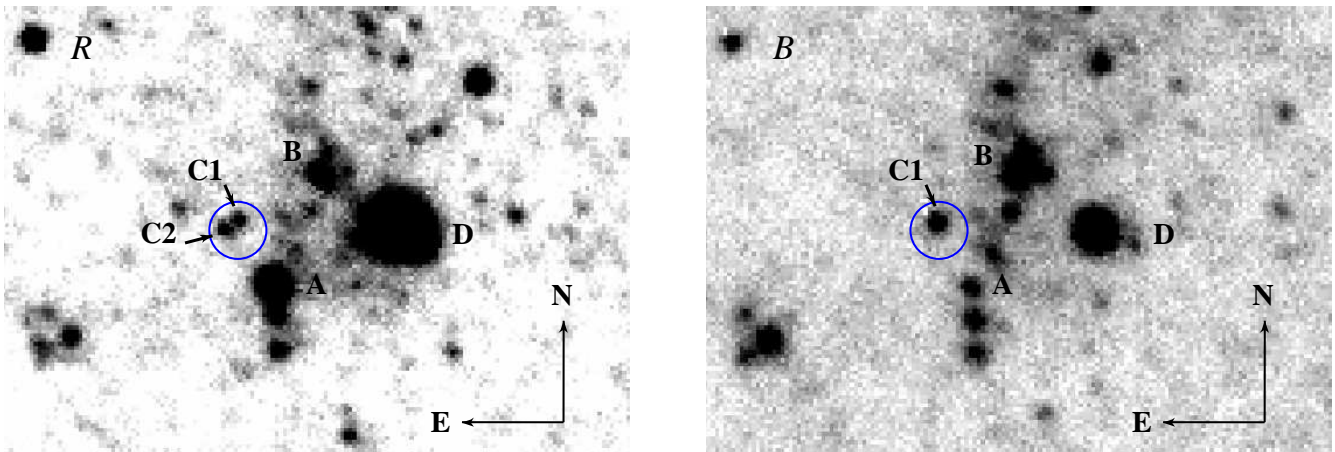


FIG. 1.— *R* (left) and *B* (right) VLT+FORIS1 images of the field around NGC 1313 X-2 ( $30'' \times 20''$ ). The circle is the  $2\sigma$  *Chandra* error-box ( $1.4''$ ). In the *R* frame, the counterpart is clearly resolved in two point sources, C1 and C2.

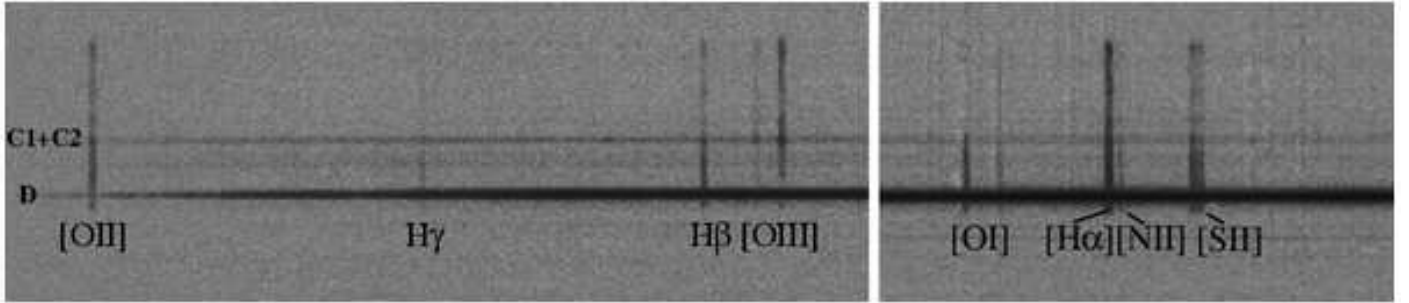


FIG. 2.— Two-dimensional spectrum (VLT+FORs1) of objects C1+C2. The slit ( $1''$ ) is oriented to include object D. The wavelength intervals are 3600-5200 Å (*left*) and 6200-7100 Å (*right*).

TABLE 1  
LOG OF THE VLT+FORs1 OBSERVATIONS.

Obs. type	Date	Filter/Grism( $\lambda_c$ )	Exp. time (s)	Seeing ( $''$ )
Image	2003-12-24	B	840×2	1.0
Image	2003-12-25	V	600×2	0.8
Image	2003-12-24	R	500×2	0.8
Spec.	2003-12-22	5900 Å	1300×2	...
Spec.	2003-12-24	5900 Å	1300×2	...
Spec.	2003-12-30	5900 Å	1300×2	...
Spec.	2004-01-15	5900 Å	1300×2	...

TABLE 2  
ASTROMETRIC POSITIONS, MAGNITUDES AND COLORS OF THE SOURCES AROUND NGC 1313 X-2 (SEE FIGURE 1).

Source	RA	DEC	B	V	R	B-V	V-R
A	03:18:21.97±0.05	-66:36:06.4±0.3	23.5±0.15	21.7±0.05	20.6±0.05	1.8±0.15	1.1±0.1
B	03:18:21.57±0.05	-66:36:00.8±0.3	22.4±0.15	22.7±0.05	22.5±0.05	-0.3±0.15	0.2±0.1
C1	03:18:22.26±0.05	-66:36:03.3±0.3	23.5±0.15	23.6±0.15	23.7±0.15	-0.1±0.2	-0.1±0.2
C2	03:18:22.36±0.05	-66:36:03.8±0.3	$\gtrsim 25.2$	24.1±0.15	23.6±0.15	$\gtrsim 1.1$	0.5±0.2
D	03:18:20.96±0.05	-66:36:03.6±0.3	20.3±0.15	18.9±0.05	18.1±0.05	1.4±0.15	0.8±0.1

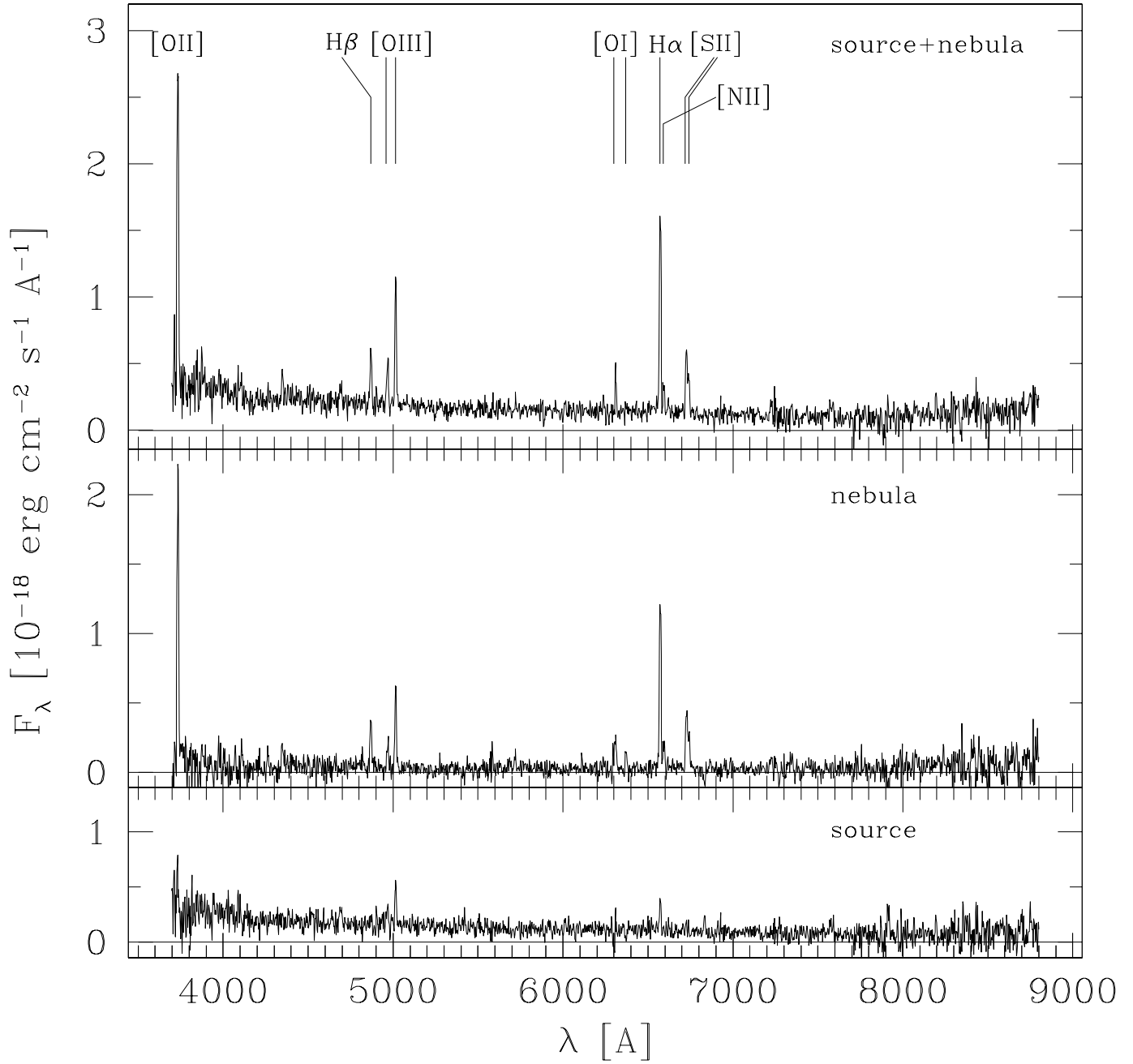


FIG. 3.— From top to bottom: VLT+FORs1 spectrum of 15 January 2004 (3700-8900  $\text{\AA}$ ), extracted from an aperture of  $2.2''$  centered on the unresolved object C1+C2; average spectrum of the nebula, extracted from two  $1''$  apertures located eastward and westward of the source position and adjacent to it; the nebula-subtracted spectrum of object C1+C2.

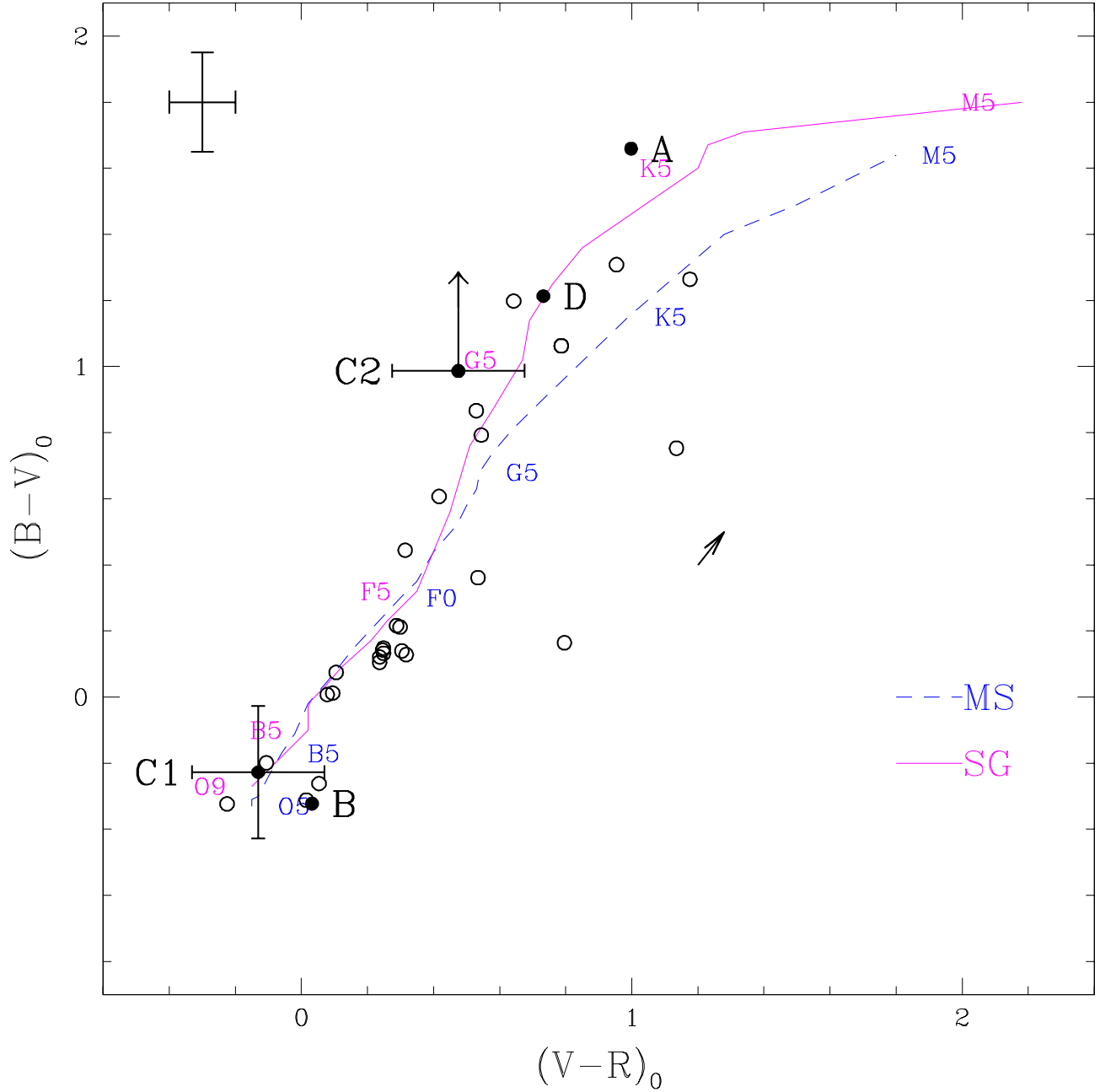


FIG. 4.—  $(B-V)_0$  vs.  $(V-R)_0$  for a sample of field objects around NGC 1313 X-2, including A, B, C1, C2 and D. Error bars are shown at the upper left corner. Measurements were corrected for Galactic extinction ( $A_V = 0.3$ ,  $E_{B-V} = 0.1$ , corresponding to a column density  $N_H = 6 \times 10^{20} \text{ cm}^{-2}$ ). The arrow indicates the reddening vector corresponding to  $E_{B-V} = 0.1$ . The solid and dashed lines represent the colors of supergiant (SG) and main sequence (MS) stars.